J Mater Sci (2010) 45:2788–2797
DOI 10.1007/s10853-010-4268-z

Study on an antifouling and blood compatible poly(ethylene–vinyl acetate) material with fluorinated surface structure

Xiao-Wen Wen · Su-Peng Pei · Hong Li · Fei Ai · Huan Chen · Ke-Yong Li · Quan Wang · Yong-Ming Zhang

Received: 29 December 2009 / Accepted: 26 January 2010 / Published online: 9 February 2010

Abstract Novel poly(ethylene–vinyl acetate) film with fluorinated surface structure was prepared via sequential surface reactions, which are alcoholysis reaction with sodium ethoxide and located fluorination reaction with 2,3,3,3-tetrafluoro-2-[1,1,2,3,3,3-hexafluoro-2-(heptafluoropropoxy)propoxy] propionyl fluoride, respectively. The obtained novel film possesses ordered perfluoroalkyl ether surface layer proved by detailed ATR-FTIR, XPS, and contact angle measurement, which substantiates the success of this new route to get better-tailored surface meeting the biological needs. Hemocompatibility of the resultant films was evaluated by hemolysis test and platelet adhesion test. The results indicated that the poly(ethylene–vinyl acetate) film surface displayed low hemolytic activity and no platelet adhesion due to its extremely low surface tension, which results from the special micro-electric field of perfluoroalkyl ether layer. The yielded transparent film with good properties exhibits a promising application prospect in biology and medical science in view of its flexible substrate and unique biocompatible surface.

Introduction

Intense effort has been being made on preparing biomedical materials through centuries because of their extensive and significant importance in biology and medicine science [1]. Generally, two fundamental requirements are proposed for biomedical materials by polymer and biology scientists from standpoints of both scientific and practical considerations. First, their physical properties such as flexibility or rigidity, mechanical strength and transparency, etc., must fulfill the purposes for multiple practices relating with biological preference. Second, the design of biomedical materials should aim at a perfect outer-layer, which could effectively and efficiently leads to blood compatibility, biocompatibility and bioactivity [2–4]. There is no doubt that their physical properties mainly depend on the bulk body structures, but their biology integrations are determined mostly by the surface structures and micro-electric fields of the chemical groups toward outside [5, 6], especially when brought into contact with particular biological elements. Hence, in the first place, a suitable polymer should be prepared or found to meet the requirement of desirable physical properties for biomedical use. Meanwhile, it is of much greater importance for scientists to design and tailor the material's outermost layer with various functional chemical groups to favorably interact with the biological elements of the organism.

Electronic supplementary material The online version of this article (doi:10.1007/s10853-010-4268-z) contains supplementary material, which is available to authorized users.

X.-W. Wen · S.-P. Pei · H. Li · F. Ai · H. Chen · Y.-M. Zhang (✉)
School of Chemistry and Chemical Engineering, Shanghai Jiao Tong University, Shanghai 200240, People's Republic of China
e-mail: ymzsjtu@yahoo.com.cn

K.-Y. Li
Shanghai First People's Hospital, Shanghai 200092, People's Republic of China

Q. Wang
National Animal Medicine Research Center, Chinese Academy of Agricultural Sciences, Shanghai 200232, People's Republic of China

Based on the very above considerations, poly(ethylene–vinyl acetate), an increasingly important and widely used thermoplastic resin, has been considered to be a good candidate for biomedical materials [7, 8] due to its good physical properties, ease of handling and processing, and moderate biocompatibility. However, the material's surface would undergo unfavorable biological response when contacting with living systems such as blood, cells, and tissues [6, 9]. Several methods have been developed to tackle this tough issue by modifying. The blood compatibility and biocompatibility of poly(ethylene–vinyl acetate) is expected to be improved by physical [10–12] or chemical [13–17] methods to fully explore its potential as biomedical materials. Particularly, functional fluorinated materials are emerging as important tools to achieve enhanced performance and higher stability under a variety of conditions in biology [18–23]. Direct chemical grafting method with fluorine-containing compound was attempted such as direct exposure materials to dangerous F_2 gas [24], fluorine-containing electrical discharges [25, 26], plasma process [27, 28], and sputter deposition [29–32]. However, some problems should be further and better resolved in how to achieve the defined surface structure and how to make the grafted groups stable on their locations. Meanwhile, continued trial to search for more effective fluorine-containing groups attached to surface is still conducted by researchers.

Based on our former work [33–35], in this study, we developed a unique route to achieve the ordered biocompatible surface by specially selecting the 2,3,3,3-tetrafluoro-2-[1,1,2,3,3,3-hexafluoro-2-(heptafluoropropoxy)propoxy] propionyl fluoride (n-$C_3F_7OCF(CF_3)CF_2OCF(CF_3)CFO$) as the functional fluorinating reactant, and prepared the surface functionalized poly(ethylene–vinyl acetate) film with perfluoroalkyl ether groups through two-steps strategy. The specially selected fluorinating agent is a kind of fluorine end-capped compound with perfluoroalkyl ether linkage, connecting the perfluoropropyl group toward outside, which is greatly known for its rather low surface energy and good oxygen compatibility [19, 36–38]. Through this functional fluorination, perfluoroalkyl ether chains with a high surface density and precise localization could be covalently bonded to the poly(ethylene–vinyl acetate) film surface, forming a new surface layer with a variety of new functional properties including oxygen compatibility, low surface energy, and exceptional chemical and biological inertness while the substrate's mechanical properties are kept at the same time. Such newly yield material is expected to present non-biofouling properties and improved blood compatibility, accordingly. In addition, its preliminary blood compatibility in vitro was further studied by hemolysis test and platelet adhesion test.

Materials and methods

Materials

Poly(ethylene–vinyl acetate) was purchased from Hyundai Co. Ltd (VS410, vinyl acetate content is 26 wt%), and Table S1 (see supporting information) lists some of its physical parameters provided by the supplier. 2,3,3,3-Tetrafluoro-2-[1,1,2,3,3,3-hexafluoro-2-(heptafluoropropoxy) propoxy] propionyl fluoride (n-$C_3F_7OCF(CF_3)CF_2OCF(CF_3)CFO$) was kindly supplied by Dongyue Shenzhou New Material Company. Toluene, ethanol, and acetone were purchased from Sino-Pharm Chemical Reagent Co. Ltd, and used as received without further purification. Water used in experiments was purified using a Millipore water purification system.

Methods

Preparation of the surface modified poly(ethylene–vinyl acetate) films

Pure poly(ethylene–vinyl acetate) granular material was cleaned by washing with purified water in an ultrasonic washer, and dried at room temperature under vacuum conditions before use. Pristine poly(ethylene–vinyl acetate) substrate film was prepared by casting from 10 wt% toluene solution onto glass wafer under 40 °C, and then was cut into 10 mm diameter circular disks for the following preparation. The film thickness was approximately 500 μm. Before surface modification, the circular samples were cleaned by washing with ethanol and purified water in sequence, and dried in vacuum at 40 °C overnight.

Surface alcoholysis was conducted by immersing the clean and dry poly(ethylene–vinyl acetate) samples into 0.588 mol/L sodium ethoxide ethanol solution under reflux conditions at 40 °C for 7 h (Scheme 1, step 1). The samples were then fully rinsed with purified water to neutral, and dried in vacuum at 37 °C for 12 h.

Surface alcoholysised poly(ethylene–vinyl acetate) samples (referred to as "H-poly(ethylene–vinyl acetate)" below) were then placed into 15 g 2,3,3,3-tetrafluoro-2-[1,1,2,3,3,3-hexafluoro-2-(heptafluoropropoxy)propoxy] propionyl fluoride at 30 °C for 3 h to carry out the fluorination reaction (by esterification), forming a functional perfluoroalkyl ether groups grafted surface. A small amount (1–2 drops) of triethylamine was added into the reaction tube at the onset of the reaction to neutralize hydrofluoric acid that was generated during the reaction (Scheme 1, step 2). The surface fluorinated samples (referred to as "F-poly(ethylene–vinyl acetate)" below) were washed with acetone repeatedly to remove the excess unreacted

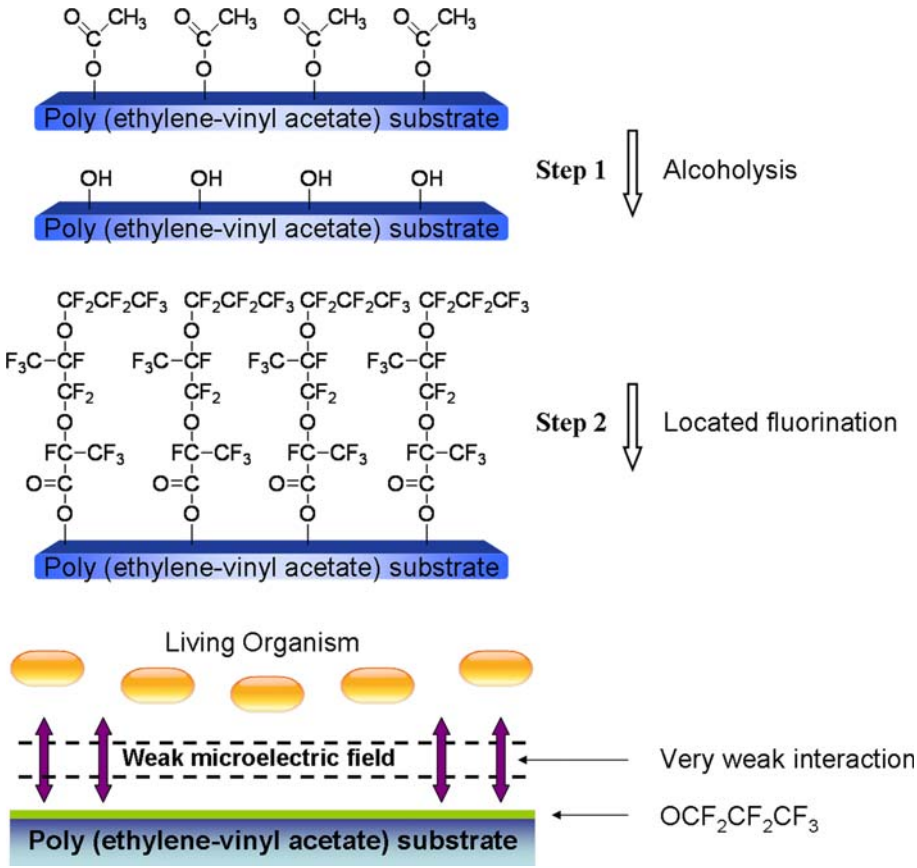

Scheme 1 Schematic illustration of surface functional fluorination on poly(ethylene–vinyl acetate) films

fluorinating agent, followed by the final wash with purified water for 1 h, then dried in vacuum at 37 °C for 24 h for blood compatibility testing and other surface analysis.

Surface analysis

To study the chemical compositions of modified poly(ethylene–vinyl acetate) film surface, the attenuated total reflectance Fourier transform infrared (ATR-FTIR) spectra were obtained using single-beam spectrometer (Bruker Tensor 27, Germany). Spectra were recorded at 4 cm^{-1} resolution and 32 scans were collected per trace.

XPS spectra for the F-poly(ethylene–vinyl acetate) film samples were recorded using a VG ESCALAB MKII multifunction spectrometer, with non-monochromatized MgKα X-rays as the excitation source. The system was carefully calibrated by Fermi-edge of nickel, Au 4*f*2/7 and Cu 2*p*2/3 binding energy. Pass energy of 70.0 eV and step size of 1.0 eV were chosen when taking spectra. In the analysis chamber pressures of 1–2 × 10^{-7} Pa were routinely maintained.

Contact angle measurement was carried out on film samples surface using a Contact Angle System OCA 20 (DataPhysics Instruments GmbH, Germany) in air at ambient temperature. The static contact angles were measured by the sessile drop method with a water drop (3 μL) being placed on the films surface. Contact angle values reported are the average of six measurements taken at different positions on each sample. The contact angle variability is within 2°.

Blood compatibility evaluation

Buffers and blood The phosphate-buffered saline (PBS) contained 8.0 g sodium chloride (NaCl), 0.2 g potassium chloride (KCl), 0.24 g potassium dihydrogen phosphate (KH_2PO_4) and 2.9 g disodium hydrogen phosphate dodeca hydrate ($NaHPO_4{\cdot}12H_2O$), pH = 7.4. The glutaraldehyde buffer contained 2.5% (v/v) glutaraldehyde in PBS, pH = 7.4.

The cleaned and dried surface modified samples were soaked into physiological saline to be equilibrated for 24 h before the blood compatibility testing. Fresh blood was drawn from healthy adult volunteers by venipuncture into acid citrate dextrose anticoagulant (ACD medium). Platelet rich plasma was kindly supplied by the Shanghai Red Cross Blood Center.

Hemolysis analysis Hemolytic activity was assessed by determining hemoglobin release under static conditions

using the two phase hemolysis test (according to ASTM F 756-00). Blood testing solution was prepared by using 4 mL fresh human blood with an ACD medium and was diluted with 5 mL of physiological saline. In the first phase, each sample was incubated in 10 mL pure saline for 30 min at 37 °C. Then, diluted fresh human blood (0.2 mL) was added and incubation went on for another 60 min in a shaker at the constant temperature of 37 °C. Positive and negative controls were produced by adding 0.2 mL of diluted fresh human blood to 10 mL of purified water and saline, respectively. After incubation, samples were centrifuged at 2500 r/min for 5 min. Optical density of the supernatant was measured at 545 nm by a spectrophotometer. The hemolysis ratio was calculated according to Eq. 1, in which Z represented the hemolysis ratio, D_t represented the absorptance of test samples, D_{nc} and D_{pc} represented the negative samples and positive samples, respectively (ASTM F 756-00).

$$Z = \frac{D_t - D_{nc}}{D_{pc} - D_{nc}} \times 100\% \quad (1)$$

Platelet adhesion tests Pristine poly(ethylene–vinyl acetate), H-poly(ethylene–vinyl acetate), and F-poly(ethylene–vinyl acetate) samples were incubated with the platelet rich plasma (PRP) for 1 h at 37 °C under static conditions. Briefly, after 1 h incubation, the samples were rinsed carefully three times with PBS buffer. The adherent platelets were fixed using 2.5% glutaraldehyde in PBS for at least 1 h, dehydrated in a graded series (50%, 60%, 70%, 80%, 90%, 95%, and 100%, v/v) of ethanol, and dried under vacuum at 37 °C overnight [10, 13]. The samples were then sputter coated with a thin layer of gold and observed using a field emission scanning electron microscopy (FE-SEM, JEOL JSM-7401F). Ten fields of vision in random were investigated to obtain the morphology and statistical result of the adherent platelets.

Results and discussion

Synthesis and surface analysis of fluorinated poly(ethylene–vinyl acetate) films

In all attempts to achieve the useful biocompatible materials, the key strategy is how to realize a surface with the desirable surface structure on the desirable substrate through elaborate design and implementation. In our study, we focused on producing a perfluoroalkyl ether outermost layer which is covalently bonded to the flexible poly(ethylene–vinyl acetate) substrate. The outside extending-$OCF_2CF_2CF_3$ groups form an ordered and packed layer which exhibits a weak micro-electric field and consequently shows very weak interactions with the contacted living organism.

Our efforts to functionalize poly(ethylene–vinyl acetate) film surface with perfluoroalkyl ether groups were based on the following approach which was conceived to be a precisely located fluorination compared with the previous methods since the as-used substrate's chemical structure and reactant unit are definite. The chemistry used here is illustrated in Scheme 1. The general idea was that a surface alcoholysis reaction of poly(ethylene–vinyl acetate) was first conducted to completely convert the surface structures from vinyl acetate (VA) units to vinyl alcohol (VOH) units to a controlled deepness, and thus created hydroxyl groups sites to carry out the following reaction for functional perfluoroalkyl ether groups' immobilization.

The ATR-IR spectra of poly(ethylene–vinyl acetate) samples subjected to the chemistry in Scheme 1 aptly illustrates the synthesis process. As can be seen in the IR spectra in Fig. 1a of poly(ethylene–vinyl acetate), there is neither hydroxyl nor perfluoroalkyl ether group on poly(ethylene–vinyl acetate) surface (Fig. 1a: aliphatic C–H 2705–3035 and 1466 cm^{-1}, ester C=O 1737 cm^{-1}, C–O–C stretch 1238 and 1025 cm^{-1}) [39]. However, after the alcoholysis treatment (Fig. 1b), the significant decrease of the vinyl acetate ester unit related peaks (1737, 1238, and 1025 cm^{-1}) and the appearance of a new broad band at 3010–3700 cm^{-1}, which is attributed to OH stretching vibration of vinyl alcohol hydroxyl unit, confirmed the presumed first step conversion. Compared to Fig. 1a, b, Fig. 1c is the spectrum of fluorinated poly(ethylene–vinyl acetate), where the OH broad band disappears and new peaks appear due to the location of perfluoroalkyl ether structures (Fig. 1c: ester C=O 1779 cm^{-1}, CF_3 stretch 1340 cm^{-1}, CF_2 stretch 1230 and 1280 cm^{-1}, CF stretch 1150 cm^{-1}, CF_2–O–F stretch 1033 and 993 cm^{-1}) [37, 40].

As we aimed to obtain a high density of functional perfluoroalkyl ether groups, the two processes illustrated in Scheme 1 were controlled by reaction time based on the conversion extent measured by surface investigation results discussed below (ATR-IR, XPS, and contact angle measurement). The strong and characteristic band at 1737 cm^{-1} in Fig. 1a, b and 1779 cm^{-1} in Fig. 1c corresponding to the carbonyl stretching (The wavenumber shift is due to the chemical structure and environment changes for fluorine atoms' stronger electronegativity.) allows a quantitative determination of the residual acetates in the first acoholysis step as well as the grafted perfluoroalkyl ether in the second fluorination step [41, 42]. Normalized IR spectra of modified poly(ethylene–vinyl acetate) at different stages for different treatment time were analyzed. After subtracting backgrounds, aliphatic C–H peaks at 2750–3050 cm^{-1} was chosen as a calibration, and the

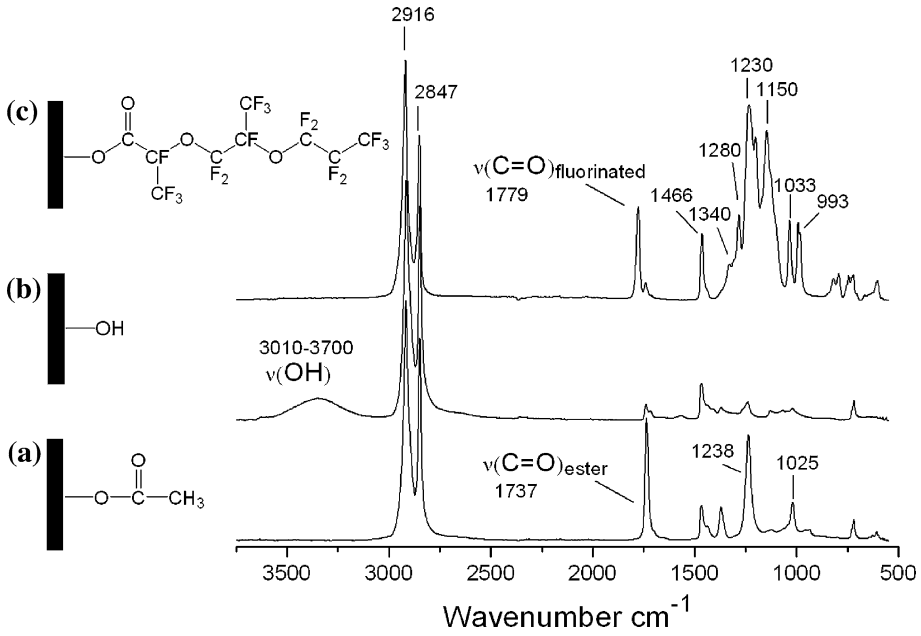

Fig. 1 ATR-FTIR spectra of pristine poly(ethylene–vinyl acetate) (*a*), H-poly(ethylene–vinyl acetate) (*b*) and F-poly(ethylene–vinyl acetate) (*c*)

integrated intensity (referred to as A) of the peaks in the 1680–1780 cm^{-1}[H-poly(ethylene–vinyl acetate)], 1750–1820 cm^{-1} [F-poly(ethylene–vinyl acetate)], and 2750–3050 cm^{-1} (C–H) regions were calculated and analyzed. $A_{H\text{-poly(ethylene–vinyl acetate)}c=o}/A_{C–H}$ and $A_{F\text{-poly(ethylene–vinyl acetate)}c=o}/A_{C–H}$ versus treatment time were plotted in Fig. 2a, b, representing the conversion extent in step one and graft density in step two, respectively. Graph in Fig. 2a shows that $A_{H\text{-poly(ethylene–vinyl acetate)}c=o}/A_{C–H}$ ratio reaches a constant value after treatment of approximately 270 min, and the similar tendency is observed in Fig. 2b demonstrating that $A_{F\text{-poly(ethylene–vinyl acetate)}c=o}/A_{C–H}$ ratio reaches the constant value after treatment of approximately 180 min. Accordingly, the surface functional fluorination was operated to achieve the highest perfluoroalkyl ether grafting density.

XPS spectroscopic studies of the F-poly(ethylene–vinyl acetate) surfaces further confirm the IR results. These results are listed in Table 1 and show that the poly(ethylene–vinyl acetate) surface after functional fluorination has reasonable elemental composition and ratio corresponding to the covering perfluoroalkyl ether structure. XPS survey scans (Fig. 3, 30° take-off angle) show that fluorine, carbon, and oxygen are present on the F-poly(ethylene–vinyl acetate) surface as expected based on their binding energy signatures. The surface concentration of fluorine is 31.7 at.%, that of carbon is 56.6 at.%, and that of oxygen is 11.2 at.%, respectively. To further quantify and identity the changes in the F-poly(ethylene–vinyl acetate) surface, detailed analysis of the high-resolution XPS spectra were carried out. Figure 4 shows the results for carbon, and Table 1 summarizes the numerical values. There were two

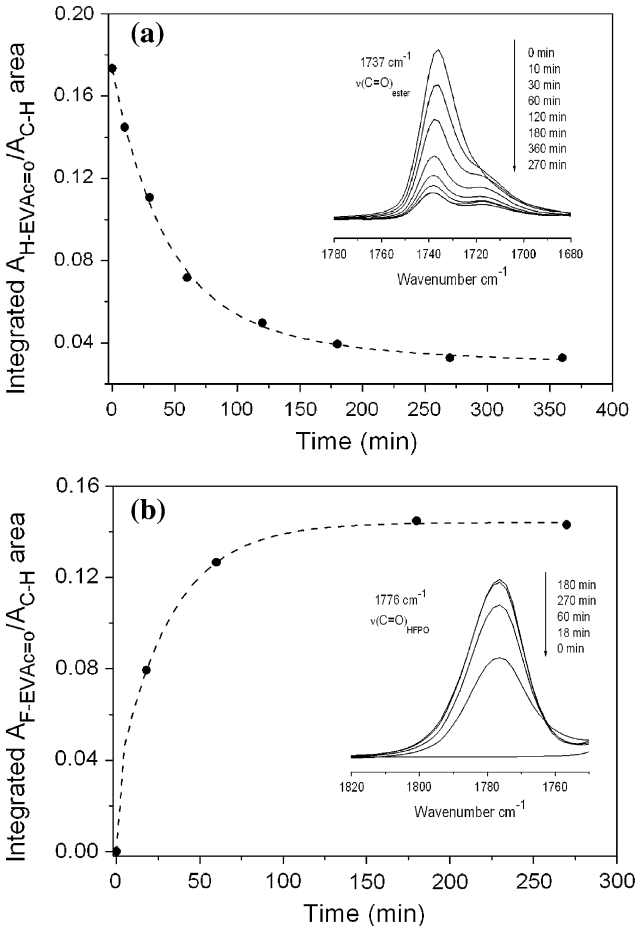

Fig. 2 **a** Integrated peak intensity ratio from ATR-IR spectra of C=O (1680–1780 cm^{-1}) to C–H (2750–3050 cm^{-1}) versus reaction time; **b** Integrated peak intensity ratio from ATR-IR spectra of C=O (1750–1820 cm^{-1}) to C–H (2750–3050 cm^{-1}) versus reaction time

Table 1 Carbon, fluorine, and different fluorinated species content with different take-off angles in XPS analysis

	Take-off angle		
	30°	50°	90°
Element (at.%)			
F	31.7	25.9	20.5
C	56.6	62.9	68.0
F/C	0.56	0.41	0.30
Species			
Binding energy (eV)/area%			
CH_2	288.1/73.8	286.1/81.1	285.9/86.1
CF	293.2/6.4	291.8/3.2	290.2/2.6
CF_2	295.2/6.9	293.0/3.3	291.7/2.1
CF_3	296.2/8.0	294.8/5.7	294.4/3.5

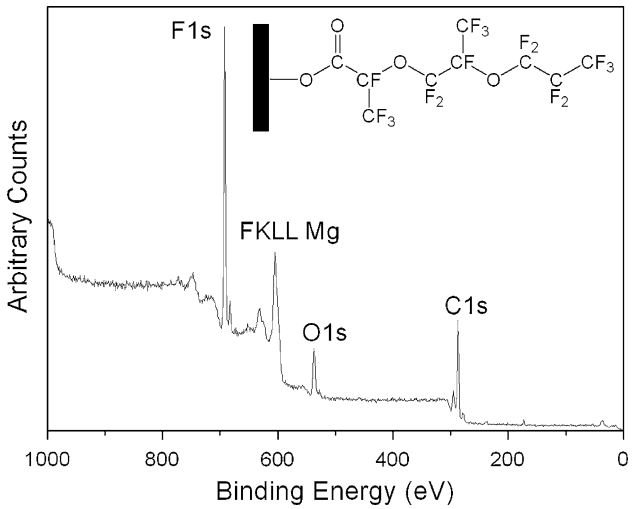

Fig. 3 XPS survey spectrum of the F-poly(ethylene–vinyl acetate)

dominant carbon peaks at the binding energies of 288.1 and 295.6 eV with a split peak at 293.2 eV, which are assigned to ethylene carbon and fluorinated carbon on the F-poly(ethylene–vinyl acetate) surface, respectively. The high-resolution XPS carbon signals in Fig. 4 can be associated with different species. The strongest component at 288.1 eV is assigned to the CH_2 groups, which are poly(ethylene–vinyl acetate) backbone carbon, while the components at 296.2, 295.2, and 293.2 eV are assigned to CF_3, CF_2, and CF groups (fluorinated carbon), respectively [43, 44]. The additional minor carbon-containing components at 289.4 eV correspond to ester carbon connected to the poly(ethylene–vinyl acetate) backbone. Hence, the resolved C1*s* peaks of the F-poly(ethylene–vinyl acetate) surface evidently explain the detailed surface chemical structures, which are consistent with the IR spectra.

There is no OH band detected in Fig. 2c after fluorination indicating the complete grafting on the surface since

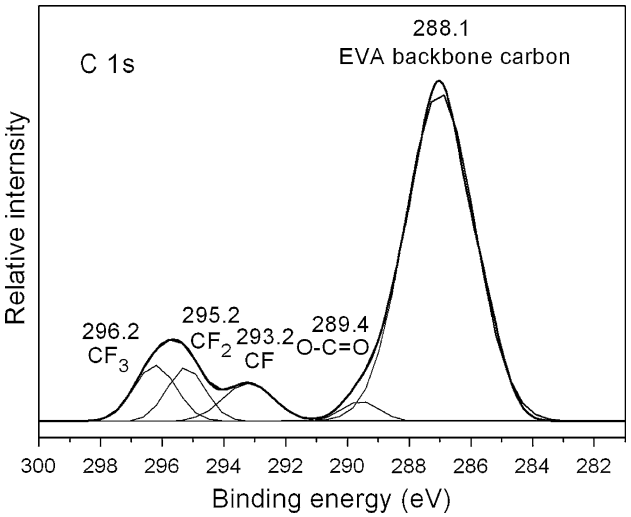

Fig. 4 Results from high resolution XPS spectra of carbon

no possible reactive site remains. In comparison with the ATR-IR method, XPS investigation is much more surface sensitive. To better investigate the surface chemistry in different depth, the same F-poly(ethylene–vinyl acetate) film was studied using XPS at three different take-off angles, which representing three depths of penetration in the range of approximately 5–10 nm [45]. Table 1 lists the element concentration of F-poly(ethylene–vinyl acetate) film. The expected fluorine concentration of the perfluoroalkyl ether surface is approximately 30.2%, and the observed real fluorine concentration is 20.5% with the take-off angle of 90°. However, the surface shows a fluorine concentration of 31.7% with the take-off angle of 30° exceeding the fluorine concentration of perfluoroalkyl ether agent, which might be due to the immigration of $OCF_2CF_2CF_3$ end groups from the subsurface to the surface. The observation that the F/C at.% ratio decreases as the detect depth increases has given an evidence of such immigration as well. Moreover, analysis of XPS spectra at three different take-off angles yielding high-resolution XPS spectra were carried out. Results are also listed in Table 1 and indicate a relatively more rapidly increasing tendency of the species concentration of CF_3 than that of CF_2 and that of CF from the subsurface to the surface. The functional fluorine groups might have a tendency to occupy the F-poly(ethylene–vinyl acetate) surface [35] and thus express the effective surface properties of hydrophobicity and water repellence, which were confirmed by the contact angle measurements.

The above ATR-IR and XPS results successfully define the outermost fluorinated layer on poly(ethylene–vinyl acetate) substrate in both structure and depth. Distinctively, the combination of very strong C–F bonds and relatively weak micro-electric field surrounded [38] makes it possible

Table 2 Water contact angles (θ_a) of the poly(ethylene–vinyl acetate) films

Material surface	Contact angle (degrees)	
	As obtained	After PBS incubation
Pristine poly(ethylene–vinyl acetate)	86 ± 1.5	86 ± 1.0
H-poly(ethylene–vinyl acetate)	57 ± 1.5	56 ± 1.5
F-poly(ethylene–vinyl acetate)	121 ± 1.0	122 ± 1.0

for the fluorinated layer to exhibit attractive anti-biofouling and bio-inertness properties, which is responsible for the extremely outstanding biocompatibility and blood compatibility that could never achieve through the sole poly(ethylene–vinyl acetate) substrate.

Contact angle analysis data (θ_a, water contact angle) of modified poly(ethylene–vinyl acetate) samples are listed in Table 2, which show that the material's surface hydrophilicity is changed as expected after different treatments. The data is consistent with the change of property and structure of the poly(ethylene–vinyl acetate) film surface, as the IR, XPS, and wettability results show. As shown in Table 2, the θ_a value depends on the surface chemistry of poly(ethylene–vinyl acetate) films. Modified poly(ethylene–vinyl acetate) has a θ_a value of 57 ± 1.5° after the alcoholysis reaction and a θ_a of 121 ± 1.5° after the functional fluorination. The increased hydrophilicity and hydrophobicity seen from these results mirror the conversion according to the chemistry shown in Scheme 1.

To analyze the influence of functional perfluoroalkyl ether groups on surface hydrophobicity from contact angles, a graph is plotted as θ_a value versus fluorination time in Fig. 5, which shows that the F-poly(ethylene–vinyl acetate) surface hydrophobicity reaches a constant level after reaction with the fluorinating agent of approximately 120 min. Evidently, the immigration tendency and thermodynamic driving force would bring the functional perfluoroalkyl ether chains to the material's surface and meanwhile keep a stable state to express related surface properties [44, 46]. Furthermore, we examined the stability in PBS buffer of this hydrophobicity expressed by functional perfluoroalkyl ether groups through contact angle measurements. Results demonstrate that incubation in PBS buffer for 1 day at 37 °C leads to no detectable changes in hydrophobicity of these films within the experimental error, and indicate the relatively stable surface chemical and physical environment after the fluorination treatment.

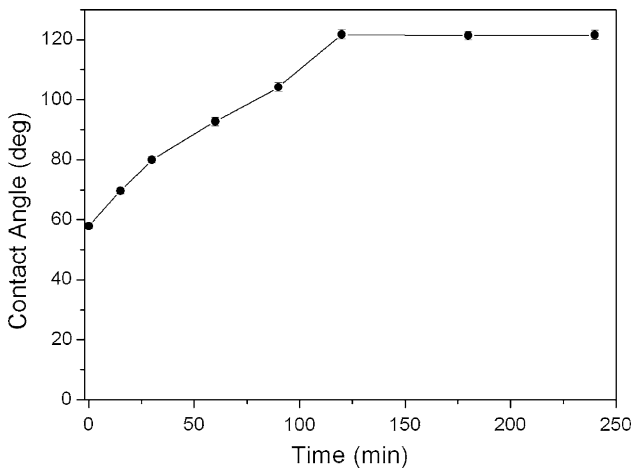

Fig. 5 Contact angles versus fluorination time on poly(ethylene–vinyl acetate) film surface

All of the above results indicate that perfect poly(ethylene–vinyl acetate) film with perfluoroalkyl ether out layer surface was successfully prepared. After the functional fluorination on poly(ethylene–vinyl acetate) film, some changes in surface oriented biological properties should accrue to the F-poly(ethylene–vinyl acetate) film. Accordingly, we conducted the hemolysis test and platelet adhesion test to evaluate its biocompatibility and blood compatibility.

Blood compatibility

Hemolysis

Hemolysis of the blood is an extremely serious problem associated with the bio-incompatibility of materials faced by biomaterials researchers. Red blood cells may hemolyze when contacting with implant materials and thus cause eventually failure [4, 47]. Therefore, in evaluating blood compatibility and biocompatibility, it is of vital importance to investigate the hemolysis ratio of the material. Here, surface modified poly(ethylene–vinyl acetate) films at different stages were selectively chosen to explore there hemolytic activity.

Results obtained from hemolysis test of ACD blood with H-poly(ethylene–vinyl acetate) and F-poly(ethylene–vinyl acetate) are shown in Table 3. According to the related standard (ASTM F 756-00), permissible hemolysis ratio of biomaterials should be at least lower than 5%. Therefore, first, the hemolysis ratio of 0.55% with pristine poly(ethylene–vinyl acetate) makes it suitable as the substrate material. As to the alcoholysised surface, a slightly less hemolysis rate was obtained in consistence with the observation by many other researchers since it is accepted that a hydrophilic surface would improve the material's compatibility to a certain extent when contacting with biofluids [48–51]. More importantly and promisingly, a key finding here is the fact that functional fluorinated surface with perfluoroalkyl ether groups is much less hemolytic than the pristine one and the

Table 3 Hemolytic activity of surface modified poly(ethylene–vinyl acetate)

Sample	Optical density at 545 nm	Hemolysis ratio (%)
Water	0.8180	100.00
Saline	0.0050	0.00
Pristine poly(ethylene–vinyl acetate)	0.0095	0.55
H-poly(ethylene–vinyl acetate)	0.0090	0.49
F-poly(ethylene–vinyl acetate)	0.0055	0.06

alcoholysised one as well according to its attractive lower hemolysis ratio of 0.06%. Therefore, leading to no damage of red blood cells, the F-poly(ethylene–vinyl acetate) film exhibits desirable blood compatibility. Previous studies [19] have also found that acute toxicity of the fluorinated substance is not more than and in fact sometimes lower than that of hydrogenated analogs.

Platelet adhesion tests

Embolic problems caused by clotting, which could result in failure of blood contacting biomedical materials, are also tough issues to be tackled among biomaterials research. During the blood clotting process, platelets (also named thrombocytes) are plasma membrane-possessed megakaryocyte fragments that play a pivotal role [4, 52]. Accordingly, in order to pursue a blood-compatible material surface, the primary responsibility is to resist platelet adhesion so as to hinder the thrombogenic cascade. In this study, in vitro platelet adhesion experiment was conducted to evaluate the blood compatibility of both pristine and modified poly(ethylene–vinyl acetate) films. Figure 6 displays scanning electron micrographs of the pristine poly(ethylene–vinyl acetate), H-poly(ethylene–vinyl acetate), and F-poly(ethylene–vinyl acetate) after exposure to platelet-rich plasma for 1 h, and the adhered platelets were assessed, accordingly.

Apparently, many fully spread and partially activated platelets adhere to the untreated poly(ethylene–vinyl acetate) film surface as shown in Fig. 6a, b. Some platelets even aggregated to form thrombus on the pristine poly(ethylene–vinyl acetate) surface. However, both H-poly(ethylene–vinyl acetate) and F-poly(ethylene–vinyl acetate) films show promising results in platelet adhesion. Platelets are less attached and keep their conformation better on the hydroxyl-containing surface shown in Fig. 6c, d, which is consistent with other studies [48–51]. Nevertheless, of the three sorts of materials, both outstanding antifouling property and blood compatibility can be clearly seen in Fig. 6e, f illustrating a much cleaner and smoother surface of F-poly(ethylene–vinyl acetate) compared with the above couples. Figure 6e, f revealed that grafted perfluoroalkyl ether layer functions for minimizing platelet adhesion on the modified poly(ethylene–vinyl acetate) surfaces, which consequently exhibits a favorable non-coagulant property.

To further discern the nature of the perfluoroalkyl ether structures on the F-poly(ethylene–vinyl acetate) surface for the successful non-coagulant property, several aspects should be taken into considerations. First, it is well-known that fluorocarbon groups are hydrophobic. So the much lower surface tension and work of adhesion would contribute to the non-fouling of platelets [28, 46, 53], which has been confirmed by the above experiments and discussions. Furthermore, recently, the polar hydrophobicity concept of fluorinated compounds is developed and such nature is responsible for the improved surface activity in biological applications [54]. Second, perfluoroalkyl ether is known for its good oxygen solubility and perfluropolyethers have been widely used in cosmetics [55]. Besides, the molecular orbital calculations in quantum chemistry have reported the specific interactions between carbon dioxide and the fluorinated substituent's groups [56, 57]. Therefore, the specific affinity to oxygen and carbon dioxide, which are critical delivering components by human blood, might impart the perfluoroalkyl ether grafted poly(ethylene–vinyl acetate) film surface with specific functions and properties. Since few studies were found associating with the bioactivity of perfluoroalkyl ether related structures, the above promising blood compatibility results highlight the detailed investigation to further exploit the materials application potentials.

Conclusions

A unique route was accomplished to improve the flexible poly(ethylene–vinyl acetate) material into non-coagulant functional film with outstanding blood compatibility via the strategy of two steps surface reactions. A thickness-controlled surface alcoholysis was successfully conducted, followed by the located fluorination. Hence, an outer-layer surface consisting of the ordered, covalently immobilized perfluoroalkyl ether was obtained. The surface layer with this structure was surrounded by a weak micro-electric field and accordingly showed very weak interaction with related living organism. Surface properties of this novel poly(ethylene–vinyl acetate) film has been characterized and correlated with the ATR-IR, XPS, and contact angle investigation. Results illustrate that the surface located fluorination is successfully conducted achieving highly ordered and densely packed perfluoroalkyl ether units, thus conferring an oxygen compatible, chemical inert, hydrophobic, non-fouling, and slippery surface layer on

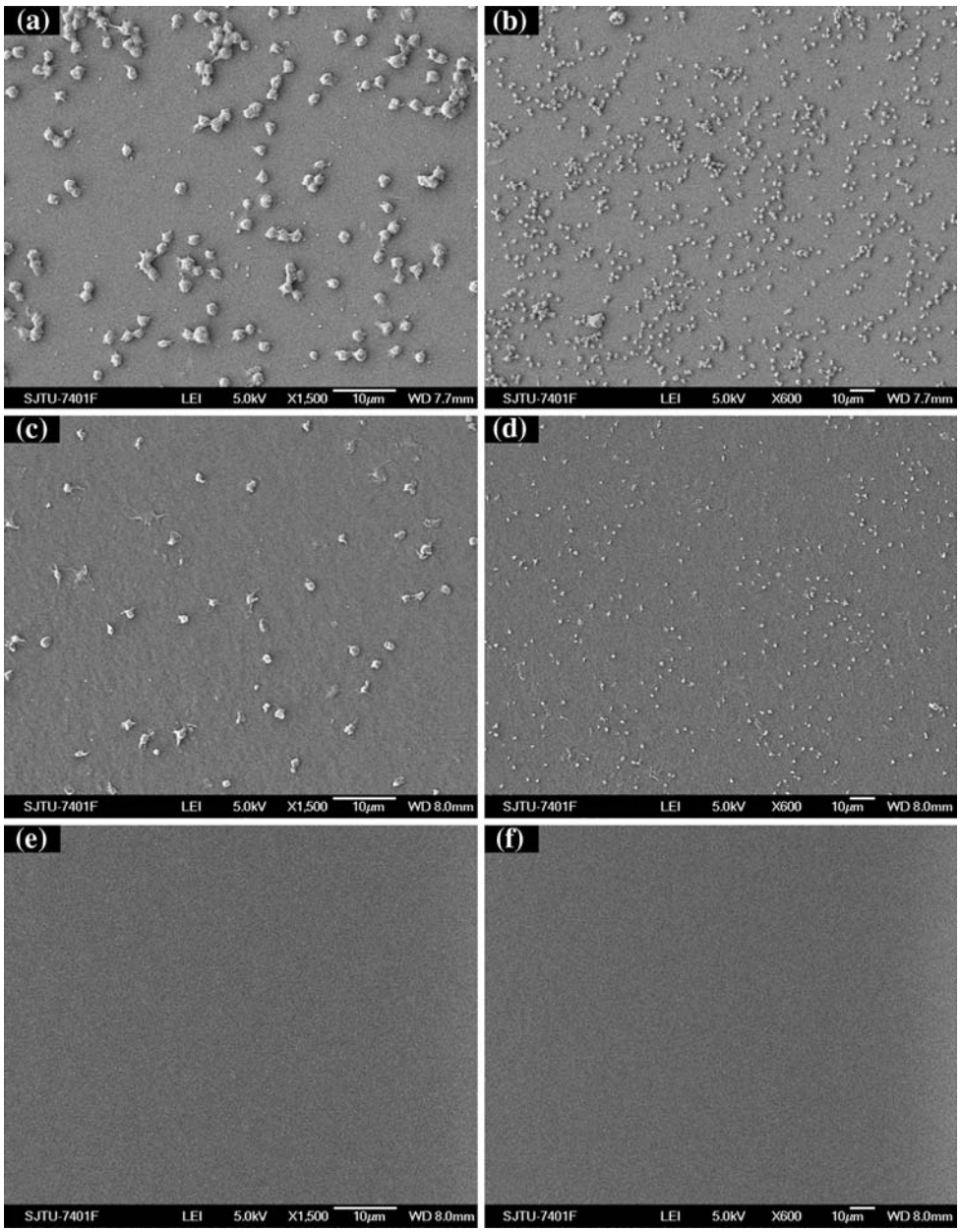

Fig. 6 Scanning electron micrographs of platelet adhesion onto pristine poly(ethylene–vinyl acetate), H-poly(ethylene–vinyl acetate), and F-poly(ethylene–vinyl acetate)

poly(ethylene–vinyl acetate) film, which exhibits an amazing improvement of blood compatibility in the following hemolysis activity test and platelet adhesion test. Such novel material with the biocompatible surface and flexible substrate could be a choice candidate for implanted biomaterial, such as artificial blood vessels in the body and blood transporting vessels outside the body. The agreeable micro-electric field of the perfluoroalkyl ether groups surrounding the outermost layer could explain the unique antifouling properties of the material, providing a guide prospective in designing new biocompatible materials in the future.

Acknowledgements This work was financially supported by the National High Technology Research and Development Program ("863" Program, No.2006AA03Z216). The authors also acknowledge Dongyue Shenzhou New Material Company for offer of materials, Ms. Wenjuan Yu in Instrumental Analysis Center of Shanghai Jiao Tong University for the help in ATR-IR test, and Dr. H. Huang at University of Connecticut for the English revision.

References

1. Tsuruta T (1996) Adv Polym Sci 126:1
2. Freier T (2006) Adv Polym Sci 203:1
3. Mao C, Qiu Y, Sang H, Mei H, Zhu A, Shen J, Lin S (2004) Adv Colloid Interface Sci 110:5

4. Ratner BD (2008) Biomaterials 28:5144
5. Uyama Y, Kato K, Ikada Y (1998) Adv Polym Sci 137:1
6. Kasemo B (2002) Surf Sci 500:656
7. Kakizawa S, Yamada K, Iino M, Watanabe M, Kano M (2003) Eur J Neurosci 17:545
8. Yin M, Yuan Y, Liu CS, Wang J (2009) Biomaterials 30:2764
9. Ratner BD (2000) J Biomater Sci Polym Ed 11:1107
10. Morimoto N, Iwasaki Y, Nakabayashi N, Ishihara K (2002) Biomaterials 23:4881
11. Zhang H, Annich GM, Miskulin J, Osterholzer K, Merz SI, Bartlett RH, Meyerhoff ME (2002) Biomaterials 23:1485
12. Shpuntoff HML, Wen MC, Singh A, Brenner N, Gambino R, Pernodet N, Isseroff R, Rafailovich M, Sokolov J (2009) Biomaterials 30:8
13. Balakrishnan B, Kumar DS, Yoshida Y, Jayakrishnan A (2005) Biomaterials 26:3495
14. Singhal JP, Ray AR (2002) Biomaterials 23:1139
15. Chen KY, Kuo JF, Chen CY (2002) Biomaterials 21:161
16. Huang N, Yang P, Cheng X, Leng Y, Zheng X, Cai G, Zhen Z, Chang F, Chen Y, Lix X, Xi T (1998) Biomaterials 19:771
17. Rossi NAA, Mustafa I, Jackson JK, Burt HM, Horte SA, Scott MD, Kizhakkedathu JN (2009) Biomaterials 30:638
18. Pagliaro M, Ciriminna R (2005) J Mater Chem 15:4981
19. Riess JG, Krafft MP (1998) Biomaterials 19:1529
20. Napier ME, Friend CM (1996) Langmuir 12:1800
21. Grondahl M, Gustafsson A, Gatenholm P (2006) Macromolecules 39:2718
22. Ernsting MJ, Bonin GC, Yang M, Labow RS, Santerre JP (2005) Biomaterials 26:6536
23. Yano M, Taketsugu T, Hori K, Okamoto H, Takenaka S (2004) Chem Eur J 10:3991
24. Clark DT, Feast WJ, Musgrave WKR, Ritchie I (1975) J Polym Sci Chem Ed 13:857
25. Corbin GA, Cohen RE, Baddour RF (1985) Macromolecules 18:98
26. Valdes TI, Ciridon W, Ratner BD, Bryers JD (2008) Biomaterials 29:1356
27. Lin JC, Tiong SL, Chen CY (2000) J Biomater Sci Polymer Ed 11:701
28. Woodward I, Schofield WCE, Roucoules V, Badyal JPS (2003) Langmuir 19:3432
29. Senesi GS, D'Aloia E, Gristina R, Favia P, d'Agostino R (2007) Surf Sci 601:1019
30. Lee EJ, Lee SH, Kim HW, Kong YM, Kim HE (2005) Biomaterials 26:3843
31. Pu FR, Williams RL, Markkula TK, Hunt JA (2002) Biomaterials 23:2411
32. Clarotti G, Schue F, Sledz J, Aoumar AAB, Geckeler KE, Orsetti A, Paleirac G (1992) Biomaterials 13:832
33. Chen H, Li H, Pei SP, Wen XW, Zhang YM (2009) Polymer 50:4317
34. Han LL, Zhang YM, Li H, Li L (2009) Colloids Surf A 334:176
35. Li H, Zhang YM, Zhang H, Xue MZ, Liu YG (2006) J Polym Sci Chem Ed 44:3853
36. Turri S, Barchiesi E (1995) Macromolecules 28:7271
37. Persico DF, Gerhardt GE, Lagow RJ (1985) J Am Chem Soc 107:1197
38. O'Hagan D (2008) Chem Soc Rev 37:308
39. Takeuchi T, Mori S (1965) Anal Chem 37:589
40. Ni HB, Li ZH, Dou HY, Li H, Zha CX (2006) J Fluorine Chem 127:1036
41. Tao G, Gong A, Lu J, Sue HJ, Bergbreiter DE (2001) Macromolecules 34:7672
42. Bureau E, Hirata Y, Cabot C, Andrio Balado A, Marais S, Saiter J (2003) J Therm Anal Calorim 71:205
43. Zhang FY, Advani SG, Prasad AK, Boggs ME, Sullivan SP, Beebe TP (2009) Electrochim Acta 54:4025
44. Ramasamy S, Pradeep T (1995) J Chem Phys 103:485
45. Jablonski A (2009) Surf Sci 603:1342
46. Anton D (1998) Adv Mater 10:1197
47. Motlagh D, Yang J, Lui KY, Webb AR, Ameer GA (2006) Biomaterials 27:4315
48. Coelho MAN, Vieira EP, Motschmann H, Mohwald H, Thunemann AF (2003) Langmuir 19:7544
49. Wang DA, Chen BI, Ji J, Feng LX (2002) Bioconjugate Chem 13:792
50. Peter K, Schwarz M, Conradt C, Nordt T, Moser M, Kubler W, Bode C (1999) Circulation 100:1533
51. Weber N, Wendel HP, Ziemer G (2002) Biomaterials 23:429
52. Rao GHR, Chandy T (1999) Bull Mater Sci 22:633
53. Jisr RM, Rmaile HH, Schlenoff JB (2005) Angew Chem Int Ed 44:782
54. Biffinger JC, Kim HW, DiMagno SG (2004) ChemBioChem 5:622
55. Scheirs J (1997) Modern fluoropolymers: high performance polymers for diverse applications. Wiley, Chichester
56. Fried JR, Hu N (2003) Polymer 44:4363
57. Ghenciu EG, Beckman EJ (1997) Ind Eng Chem Res 36:5366